

Investigation of the solidification behavior of $\text{Al}_2\text{O}_3/\text{YAG}/\text{YSZ}$ ceramic *in situ* composite with off-eutectic composition

Haijun Su*, Jun Zhang, Kan Song, Lin Liu, Hengzhi Fu

State Key Laboratory of Solidification Processing, Northwestern Polytechnical University, Xi'an 710072, PR China

Available online 5 August 2010

Abstract

Directionally solidified $\text{Al}_2\text{O}_3/\text{YAG}/\text{YSZ}$ ceramic *in situ* composite is an interesting candidate for the manufacture of turbine blade because of its excellent mechanical property. In the present study, two directionally solidified hypoeutectic and hypereutectic $\text{Al}_2\text{O}_3/\text{YAG}/\text{YSZ}$ ceramic *in situ* composites are prepared by laser zone remelting, aiming to investigate the solidification behavior of the ternary composite with off-eutectic composition under high-temperature gradient. The results show that the composition and laser scanning rate significantly influence the solidification microstructure. The ternary *in situ* composite presents ultra-fine microstructure, and the eutectic interspacing is refined with the increase of the scanning rate. The $\text{Al}_2\text{O}_3/\text{YAG}/\text{YSZ}$ hypoeutectic ceramic displays an irregular hypoeutectic network structure consisting of a primary $\text{Al}_2\text{O}_3/\text{YAG}$ binary eutectic and fine $\text{Al}_2\text{O}_3/\text{YAG}/\text{YSZ}$ ternary eutectic. Only at low scanning rate, homogeneous ternary eutectic-like microstructures are obtained in the hypoeutectic composition. Meanwhile, the $\text{Al}_2\text{O}_3/\text{YAG}/\text{YSZ}$ hypereutectic ceramic shows homogeneous eutectic-like microstructure in most cases and the eutectic interspacing is finer than the ternary eutectic. Furthermore, the formation and evolution mechanism of the off-eutectic microstructure of the ternary composite are discussed.

© 2010 Elsevier Ltd. All rights reserved.

Keywords: Ceramic eutectic; *In situ* composite; Solidification behavior; Laser zone remelting

1. Introduction

At present, environment protection and energy saving have become increasing global international problems that mankind has to face in 21st century. In order to improve the thermal efficiency and reduce the polluting emissions such as CO_2 and NO_x , considerable efforts have been devoted to developing new high-temperature structural materials with excellent mechanical properties at the temperature over 1923 K in the oxidizing atmosphere.^{1–3} Over the past few decades, directionally solidified (DS) oxide eutectic ceramic *in situ* composites have been intensively explored as potential candidates for hot-section components in advanced engines and gas turbines owing to their excellent and unique combination of high melting points, low density, retained strength at elevated temperatures, as well as superior oxidation and creep resistance.^{4–8} For examples,

in comparison with Ni-based superalloy, the use temperature of DS $\text{Al}_2\text{O}_3/\text{YAG}$ eutectic for turbine blade application can be high over 1873 K without additional cooling⁴; compared to SiC and Si_3N_4 based ceramics, DS $\text{Al}_2\text{O}_3/\text{YAG}$ eutectic remains stable at temperatures higher than 1973 K in oxidizing atmosphere.⁹ Of particular comparing with sintered oxide ceramics, directional solidification effectively removes grain boundaries and amorphous phases, allows size control over the final microstructure, contains a huge amount of clean interfaces and consequently, improving the mechanical properties.¹⁰ As a result, several DS binary oxide eutectics such as $\text{Al}_2\text{O}_3/\text{YAG}$, $\text{Al}_2\text{O}_3/\text{GdAlO}_3$, $\text{Al}_2\text{O}_3/\text{Er}_3\text{Al}_5\text{O}_{12}$ and $\text{Al}_2\text{O}_3/\text{ZrO}_2$ systems have been systematically developed and studied.⁶ However, it is of low fracture toughness ($\sim 2 \text{ MPa M}^{1/2}$) of these materials,¹¹ which extremely hinders their development as practical structural applications.

To enhance the limited toughness of DS oxide eutectic ceramics, the concept of amending phase interface bonding and altering crack path by introducing a third phase to binary eutectics has recently been used.^{12,13} It has been reported that the $\text{Al}_2\text{O}_3/\text{YAG}/\text{YSZ}$ ternary eutectic prepared by rapid solidification technique presents a much more improved toughness ($\sim 8\text{--}9.0 \text{ MPa M}^{1/2}$).^{14,15} This thus leads to renewed interest

* Corresponding author at: State Key Laboratory of Solidification Processing, Northwestern Polytechnical University, School of Materials Science and Engineering, P.O. Box 543#, Xi'an, Shaanxi 710072, PR China. Tel.: +86 29 88494825; fax: +86 29 88494080.

E-mail address: shjnpu@yahoo.com.cn (H. Su).

on the $\text{Al}_2\text{O}_3/\text{YAG}/\text{YSZ}$ ternary eutectics. So far several studies on the microstructure and mechanical properties of DS $\text{Al}_2\text{O}_3/\text{YAG}/\text{YSZ}$ ternary eutectics have been investigated.^{13–17} However, previous studies were mainly focused on the ternary eutectic composition. Few reports referred to the ternary off-eutectic composition.^{18–20} It is known that eutectic growth composition is generally not a fixed point but a range in eutectic system, and the off-eutectic composition material is more often used in practice. Moreover, homogeneous eutectic structure can also be produced at the off-eutectic composition if suitable growth conditions are selected.²¹ In this case, the coupled growth zone is possibly enlarged. Thus, the off-eutectic composite favors to produce fine homogeneous eutectic microstructure at various compositions and a broad growth rate range. Far more important is that it can freely adjust the volume fraction of eutectic phase in reinforced composite applications. For example, the mechanical properties of composites would be improved because the materials could have the best volume ratio of each component. The control of pore volume fraction in porous materials formed by removing one phase in microstructure would be also possible.²² Recently, we have investigated the microstructures and mechanical properties of the ternary composite at a hypoeutectic composition.²³ Nevertheless, a systematic research on the solidification behavior of the ternary composite with different off-eutectic compositions at a large range is little done yet, which limits sufficient understanding of the complex solidification behavior of the ternary oxide eutectic system and further optimization of the outstanding mechanical properties.

Furthermore, DS oxide eutectic ceramics generally have very high melting points (>1973 K). Using conventional directional solidification method to prepare them is difficult and leads to large eutectic spacing due to low temperature gradient.^{4,6} Recently, laser zone remelting has been successfully used to produce DS oxide eutectic ceramic composites with advantages of nonexistence of crucible, high melting temperature, large thermal temperature gradient ($>10^4$ K/cm), as well as high growth rates and low costs.^{15,19,24,25} Particularly, an additional advantage of this method over the floating zone method is the possibility to produce large areas of directionally solidified eutectics.²⁵ In this present study, two directionally solidified hypoeutectic and hypereutectic ternary $\text{Al}_2\text{O}_3/\text{YAG}/\text{YSZ}$ ceramic *in situ* composites are prepared by laser zone remelting. The microstructure characteristic and evolution of the ternary oxide composite are studied in detail to investigate the solidification behavior.

2. Experimental procedure

For laser zone remelting experiments, two off-eutectic compositions were utilized according to the ternary oxide phase diagram.²⁶ One was hypoeutectic composition with 71.1 mol% Al_2O_3 , 16.8 mol% Y_2O_3 and 12.1 mol% ZrO_2 (<18.6), and the other was hypereutectic composition with 64.6 mol% Al_2O_3 , 15.3 mol% Y_2O_3 and 20.1 mol% ZrO_2 (>18.6). The ternary eutectic composition is 65.8 mol% Al_2O_3 , 15.6 mol% Y_2O_3 and 18.6 mol% ZrO_2 . These compositions span three typical composition zones in the ternary oxide

system. Highly pure ($>4\text{N}$) commercial Al_2O_3 , Y_2O_3 and ZrO_2 nano-powders were used for the starting materials. The oxide powders were mixed with above off-eutectic compositions by wet ball milling in an aqueous solution of polyvinyl alcohol. The obtained slurry was then dried at 473 K in air for 1 h to remove the ethanol. The two powder mixtures were uniaxially pressed at 25 MPa for 10 min and then sintered at 1773 K for 2 h to obtain ceramic precursors of Φ 7 mm \times 60 mm rods and 68 mm \times 7 mm \times 5 mm plates.

Laser zone remelting was performed in a vacuum environment using a 5 kW CO_2 laser as a heating source. Under the high-energy laser beam, the sample was rapidly remelted and solidified just behind the melting zone. At the same time, the sample was moved by the numerically controlled worktable with 5-axis and 4-direction coupled motion to realize the laser beam scanning along the sample axis. To avoid composition volatilization and pores during remelting, the Ar gas is filled into the vacuum chamber from the bottom and top of samples with a flow rate of 10 L/min. The quenched solid–liquid interface was obtained by abruptly turning off the laser and the scanning speed. Further detailed processing procedure has been described elsewhere.^{19,27} The laser power used was 190–220 W, the laser beam diameter was 4 mm, and the laser scanning rate was in the range of 10–2000 $\mu\text{m}/\text{s}$.

The crystallographic phase analyses of the as-solidified samples were examined using X-ray diffraction (XRD, Rigakumsg-158) and energy disperse spectroscopy (EDS, Link-Isis). The microstructures of the samples were observed by scanning electron microscopy (SEM, JSM-5800). Quantitative calculation of the phase volume fraction was performed by digital image analysis software of SISC IAS V 8.0.

3. Results and discussion

3.1. Typical solidification microstructure

The DS ternary hypereutectic and hypoeutectic *in situ* composites present smooth surface and high density in diameter of 4–6 mm and thickness of 0.5–3 mm. The depth of the laser melt-pool is determined by the input of the laser energy, i.e., laser power density and scanning rate. Moreover, the wavy-shaped surface is also observed at high scanning rates, which may be attributed to the Marangoni effect and liquid flow due to the temperature variation at the melt-pool surface. There are no bubbles observed in the solidified samples by filling Ar gas during remelting. Fig. 1a and c shows the typical microstructures of the traversal sections of ternary $\text{Al}_2\text{O}_3/\text{YAG}/\text{YSZ}$ hypoeutectic and hypereutectic composite grown at the scanning rate of 40 $\mu\text{m}/\text{s}$, respectively. For comparison, the laser remelted $\text{Al}_2\text{O}_3/\text{YAG}/\text{YSZ}$ ternary eutectic composites grown at the same growth conditions are shown in Fig. 1b. The XRD and EDS analyses show that the DS ternary hypoeutectic and hypereutectic composites consist of three dispersed phases of Al_2O_3 , YAG and cubic yttria-stabilized zirconia (YSZ), and there are no other phases such as $\text{Y}_4\text{Al}_2\text{O}_9$ and YAlO_3 . The dark phase is Al_2O_3 , the grey phase is YAG, and the relative small white phase is YSZ. The contents of Y_2O_3 dissolved in ZrO_2 in hypoeutectic, hyper-

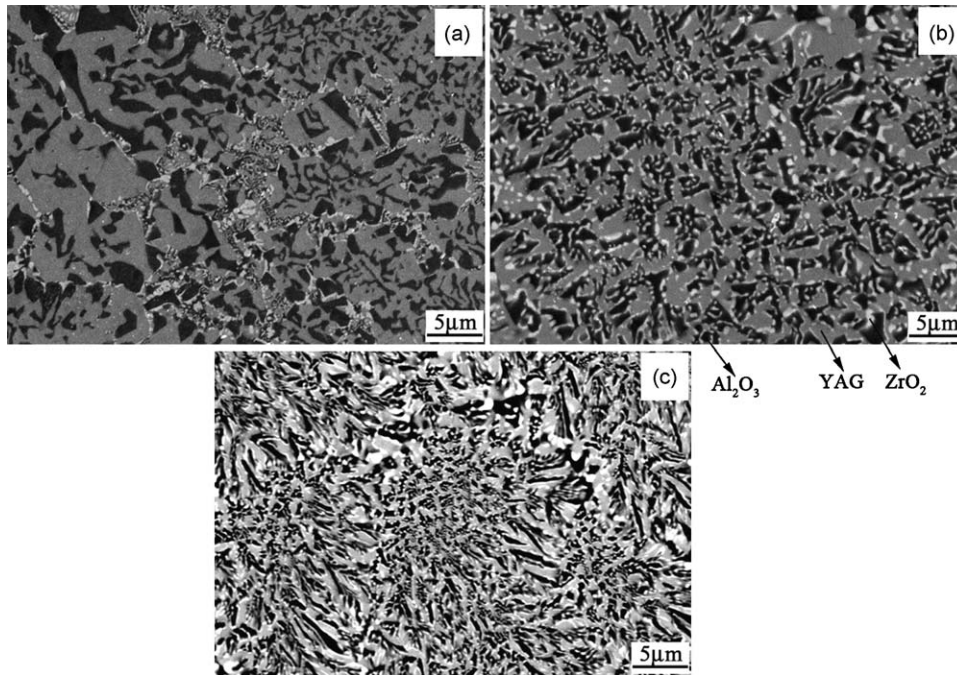


Fig. 1. Typical solidification microstructures of the laser remelted $\text{Al}_2\text{O}_3/\text{YAG}/\text{ZrO}_2$ ternary ceramic composite grown at the laser scanning rate of $40 \mu\text{m/s}$: (a) ternary hypoeutectic; (b) ternary eutectic; (c) ternary hypereutectic.

eutectic and eutectic are 8.1 mol%, 12.7 mol% and 13.3 mol%, respectively, similar to the report of Echigo et al.²⁸ In the ternary hypoeutectic ceramic, the microstructure presents a typical off-eutectic microstructure with three-dimensional network structure, consisting of a coarse primary crystal ($\text{Al}_2\text{O}_3/\text{YAG}$ binary eutectic) and a fine $\text{Al}_2\text{O}_3/\text{YAG}/\text{YSZ}$ ternary eutectic, as shown in Fig. 1a. The distribution of YSZ phase is not homogeneous, and tends to partly scatter at the $\text{Al}_2\text{O}_3/\text{YAG}$ interface or at the edge of the YAG phase, similar to the $\text{Al}_2\text{O}_3/\text{YAG}/\text{YSZ}$ ternary quasi-eutectic composites.²⁹ The volume fractions of three component phases measured by digital SEM images are 41% Al_2O_3 , 49% YAG and 10% YSZ, respectively, which is consistent with that expected for hypoeutectic composition. In contrast to the hypoeutectic composite, the microstructure of the hypereutectic composite shows a typical fine eutectic-like lamella structure similar to ternary eutectic structure (Fig. 1b), in which Al_2O_3 and YAG lamellae are interconnected, and the overfull ZrO_2 phases with spherical and lamellar shapes are mainly dispersed at the $\text{Al}_2\text{O}_3/\text{YAG}$ interface or in Al_2O_3 phase, as shown in Fig. 1c. The volume ratio of three phases is 34% Al_2O_3 /45% YAG/21% ZrO_2 . Comparing three kinds of microstructures, it is found that at the same growth conditions the interphase spacing is gradually decreased as the composition changes from hypoeutectic to eutectic and then to hypereutectic composition. It suggests that the addition of the third component can effectively refine the microstructure and, consequently improving the mechanical properties.¹⁴ Moreover, in comparison with regular eutectic metal alloys, the above off-eutectics exhibit an obvious irregular structure resulted from the faceted growth habits of eutectic phases with relation of high entropies of fusion.¹⁵ In addition, the microstructures in the three ternary composites all present a gradual refinement from the bottom to

the remelted surface due to the changes of temperature gradients, similar to the reports in the binary oxide eutectics.^{30,31}

3.2. Microstructure evolution

In the laser zone remelting, the microstructure evolution is mainly controlled by the laser scanning rate.^{19,24} Increasing the laser scanning rate can result in a significant change in the ternary composite growth. Fig. 2 shows the SEM micrographs of the longitudinal sections of the ternary hypoeutectic ceramics grown at different laser scanning rates from 15 to $1500 \mu\text{m/s}$. At low scanning rate of $15 \mu\text{m/s}$, the hypoeutectic composite presents a typical off-eutectic microstructure (Fig. 2a) consisting of an evenly dispersed coarse primary $\text{Al}_2\text{O}_3/\text{YAG}$ eutectic and a fine ternary eutectic crystal, similar to a cellular structure observed in the Y_2O_3 doped $\text{Al}_2\text{O}_3/\text{ZrO}_2$ eutectic.⁵ Increasing the laser scanning rate to $150 \mu\text{m/s}$ leads to the reduction of the cellular hypoeutectic microstructure and the formation of dendrite microstructure (as arrows show) with relative irregular array (Fig. 2b). The dendrite structure observed is never found in the DS ternary eutectic and $\text{Al}_2\text{O}_3/\text{YAG}$ binary eutectic.⁶ When the laser scanning rate further increases to $1500 \mu\text{m/s}$, the hypoeutectic ceramic shows complex dendrite structure (as arrows show) with random distribution (Fig. 2c). The produce of the cellular and dendrite structure in the ternary hypoeutectic composite can be primarily attributed to constitutional undercooling caused by the composition enrichment of the relative few ZrO_2 addition. At the high scanning rate (Fig. 2c), the formation of the random dendrite structure array is associated with the formation of a curving melt-pool with different orientation of a liquid/solid interface relative to the sample surface.³² Furthermore, as the laser scanning rate increases from 15 to $1500 \mu\text{m/s}$,

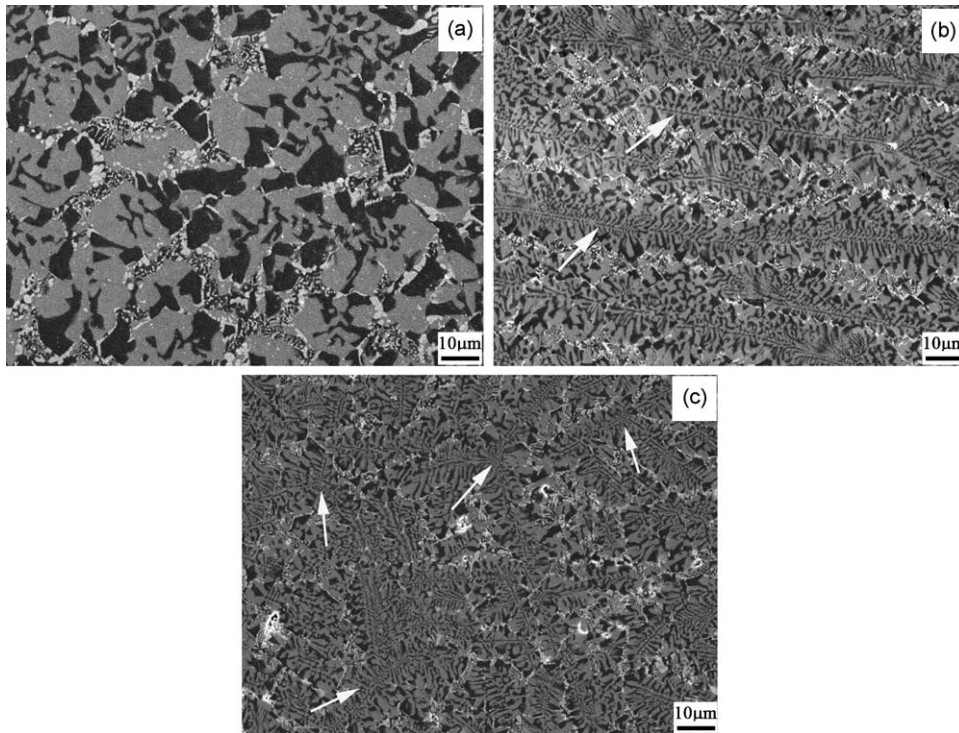


Fig. 2. SEM micrographs of the longitudinal sections of the ternary hypoeutectic ceramics grown at different laser scanning rates: (a) 15 $\mu\text{m/s}$; (b) 150 $\mu\text{m/s}$; (c) 1500 $\mu\text{m/s}$.

the interphase spacing is rapidly refined, decreasing from 3.1 to 0.3 μm . In contrast to ternary hypoeutectic composite, the ternary hypereutectic composite presents a very fine eutectic-like lamella structure. With increasing the laser scanning rate, the interphase spacing is extremely decreased (Fig. 3a–c). When the scanning rate reaches 400 $\mu\text{m/s}$, the eutectic spacing is as fine

as 100 nm, which is 1/20 of that of the ternary eutectic available obtained using the Bridgman method,¹⁸ and is almost 1/3 of the value obtained in ternary eutectic rods grown at the same conditions,¹⁵ contributing to improving mechanical properties. Moreover, Fig. 3 reveals that the eutectic-like microstructure is not modified when the laser scanning rate increases and persists

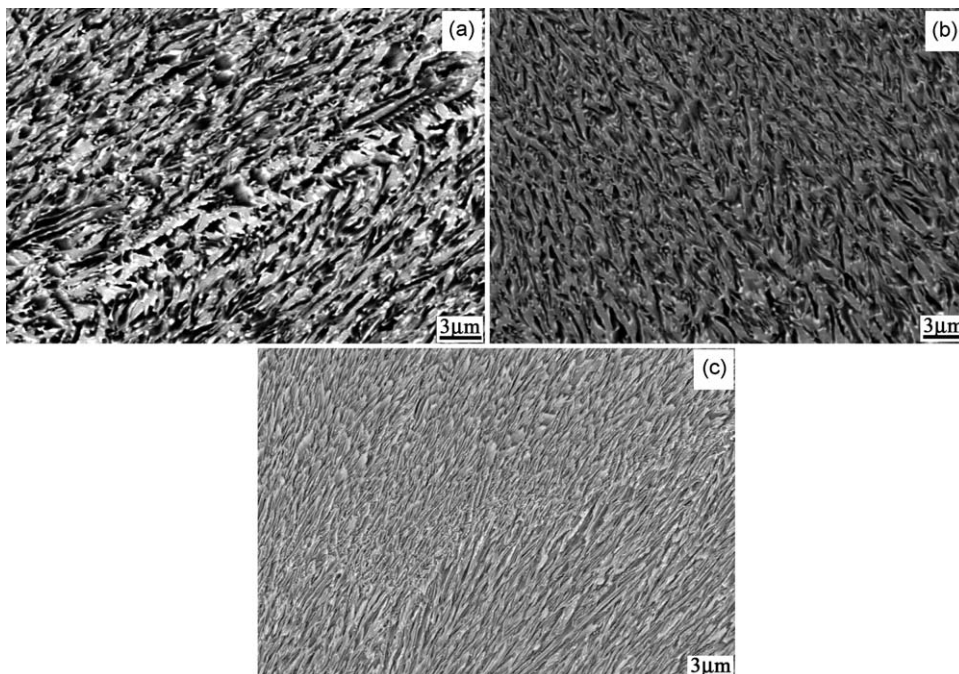


Fig. 3. SEM micrographs of the longitudinal sections of the ternary hypereutectic ceramics grown at different laser scanning rates: (a) 10 $\mu\text{m/s}$; (b) 80 $\mu\text{m/s}$; (c) 400 $\mu\text{m/s}$.

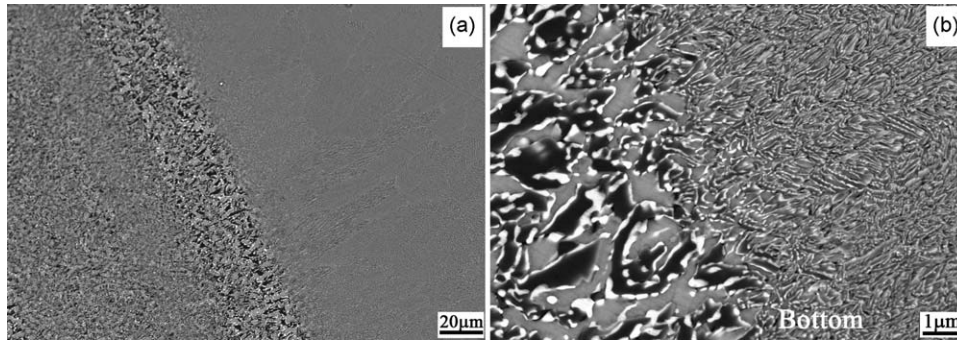


Fig. 4. Solidification interface micrograph of the ternary hypereutectic ceramics grown at the laser scanning rate of 20 $\mu\text{m/s}$ (a) and (b) the detail of the solidification interface in (a). The right zone is the quenched melt zone.

up to the rates close to 400 $\mu\text{m/s}$. The cellular microstructure is only found at the local zone of the sample at the rate of 400 $\mu\text{m/s}$, and no dendrite structure is observed. Similar result is also obtained in the laser floating zone melted $\text{Al}_2\text{O}_3/\text{YAG}$ eutectics.⁸ The analysis indicates that addition of the ZrO_2 can importantly influence the microstructure evolution and morphology characteristic.

3.3. Solidification interface characteristic

It is well known that the solid–liquid interface morphology in directional solidification process plays an important role on the microstructure transition. Well-aligned eutectic structure requires a dendrite-free planar solid–liquid interface. According to constitutional supercooling theory,³³ a planar solidification interface can be obtained when $G/R_s \geq \Delta T/D$, where G is the temperature gradient, R_s is the solidification rate, ΔT is the crystallization temperature range and D is the inter-diffusion coefficient. Laser zone remelting process produces very high-temperature gradient ($>10^4$ K/cm), providing such favorable G/R_s values. Large numbers of previous experiments about solid/liquid interface morphology were mainly focused on metals and plastic crystals, which are nearly isotropic or have sufficiently small anisotropy so that the interface does not appear faceted planes. Few studies are carried out for highly faceted oxide ceramics. In the DS ternary oxide composites, the Al_2O_3 and YAG present strong faceted growth, and the ZrO_2 presents a weak-faceted growth, which will importantly affect the formation of the planar solidification interface. In the present study, the solid/liquid interface morphology is obtained by zero power method, i.e., both the laser power and the scanning rate is abruptly adjusted to be zero when the crystal growth tends to be stable, then the solid/liquid interface morphology is attained. Fig. 4a shows the interface between the quenched and normally solidified zone in the ternary hypereutectic grown at 20 $\mu\text{m/s}$, and a detail of the solidification interface is shown in Fig. 4b. The YAG phases keep ahead to entering into the melt, playing a leading role in the melt growth. The solidification front is macroscopically curved and convex towards the solidified zone, which leads to changes of the solidification direction and the solidification rate with respect to the distance to the sample surface. The solidification direction gradually changes and the microstructure decreases from the bottom to the surface. However, in fact,

the solidified lamellae always grow perpendicular to the solidification front, namely, forming a planar solid/liquid interface, as shown in Fig. 4b. So, the eutectic-like microstructure is preferred to be formed. The interface stability is also affected by the solute diffusion.³⁴ When the steady effect of temperature gradient can not totally overcome the unsteady effect caused by solute diffusion, the interface will be unstable and dependent of the solidification rate. In the ternary hypoeutectic, the relative few addition of ZrO_2 prefers to produce the solute enrichment causing the interface instability. Consequently, with increasing the laser scanning rate, the cellular and dendrite microstructure are produced.

3.4. Production of ternary eutectic microstructure

Generally, the microstructure of the off-eutectic composition system consists of coarse primary crystals and a fine eutectic microstructure.³⁵ If a fully eutectic-like structure devoid of any cellular and dendritic regions could be obtained at off-eutectic composition, a variety of useful properties may be obtained. For example, homogeneous $\text{Al}_2\text{O}_3/\text{YAG}$ eutectic microstructure without coarse primary crystals has been achieved at the off-eutectic composition by Harada et al.²⁰ using the rapid quenching and heat treat technique. So one of the important aims of this work is to broaden ternary eutectic solidification range by studying the solidification behavior of the ternary off-eutectic system. In the present ternary hypoeutectic system, it is found that when laser scanning rate is low than 5 $\mu\text{m/s}$, the uniform ternary eutectic-like microstructures with lamellar structure can be obtained in local zone, as shown in Fig. 5a. On the contrast, in the ternary hypereutectic composite, the homogeneous eutectic-like microstructure can be thoroughly obtained at relative high laser scanning rate, as shown in Fig. 5b. The typical lamellar eutectic-like microstructure is well observed in the ternary hypereutectic ceramic grown at the high laser scanning rate of 200 $\mu\text{m/s}$. This further indicates that the stability of the solidification interface of the presented ternary hypereutectic ceramic is obviously higher than the ternary hypoeutectic one. Similar phenomena are also found in the binary oxide eutectics. In the $\text{Al}_2\text{O}_3\text{--Y}_2\text{O}_3$ binary eutectic, it is found that the coupled growth zone tends to be at the Y_2O_3 -rich side (hypereutectic point)³⁶; in the $\text{Al}_2\text{O}_3\text{--ZrO}_2$ binary eutectic, the cellular dendrites of Al_2O_3 and faceted eutectic colonies more prefer to

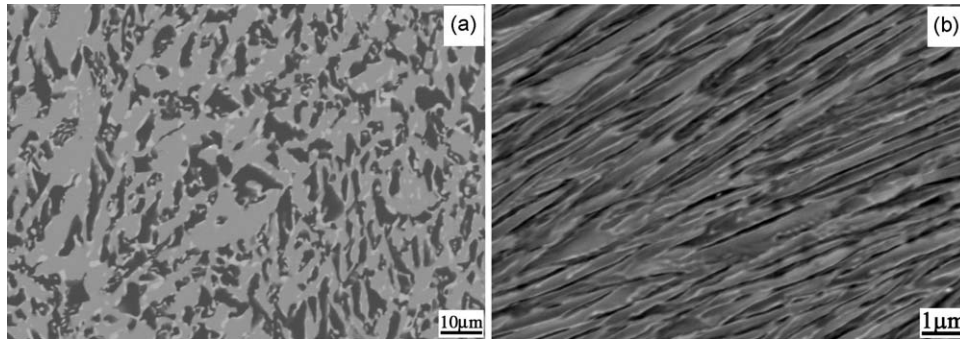


Fig. 5. Homogeneous ternary eutectic structures obtained in the ternary hypoeutectic ceramic grown at the laser scanning rate of 5 $\mu\text{m/s}$ (a) and hypereutectic ceramic grown at the laser scanning rate of 200 $\mu\text{m/s}$ (b).

appear in the hypoeutectic than hypereutectic ceramics.³⁷ So it is believed that the fine homogeneous eutectic microstructure having various volume ratios of each component at the off-eutectic compositions will produce more useful properties and applications, which are in progress.

4. Conclusions

Directionally solidified $\text{Al}_2\text{O}_3/\text{YAG}/\text{ZrO}_2$ ternary hypoeutectic and hypereutectic ceramic *in situ* composites have been produced by the laser zone remelting. The solidification behaviors of the ternary off-eutectic systems under high-temperature gradient are investigated in detail. The ternary hypoeutectic ceramic consists of a primary $\text{Al}_2\text{O}_3/\text{YAG}$ binary eutectic and fine $\text{Al}_2\text{O}_3/\text{YAG}/\text{ZrO}_2$ ternary eutectic; while the ternary hypereutectic ceramic presents a very fine homogeneous eutectic-like microstructure. The Al_2O_3 and YAG exhibit an obvious faceted growth and the ZrO_2 shows a weak-faceted growth. With increasing the laser scanning rate, the interphase spacing is rapidly decreased. Meanwhile, the morphology of the hypoeutectic composite changes from uniform hypoeutectic microstructure to cellular microstructure to dendrite microstructure and to complex dendrite but the morphology of the hypereutectic one does not change. Furthermore, the solidification interface characteristic is examined. The solidification interface stability of the presented ternary hypereutectic ceramic is obviously higher than the ternary hypoeutectic one. The homogeneous ternary eutectic-like microstructure can only be obtained at low laser scanning rate in the ternary hypoeutectic composite but can still be obtained at high scanning rate in the ternary hypereutectic one. This foundational investigation favors us to enlarge the eutectic solidification range of the ternary ceramic composite and to develop new useful properties and applications.

Acknowledgments

The authors gratefully acknowledge the National Natural Science Foundation of China (50772090), the Foundation Research Fund of Northwestern Polytechnical University (NPU-FFR-G9KY1016), the Opening Project of State Key Laboratory for Advanced Metals and Materials (2007AMM004), the Scien-

tific Research Start-up Foundation for Outstanding Persons in Northwestern Polytechnical University (GAKY3006), and the Provincial Natural Science Foundation of Shaanxi Province, and the New People and New Directions of School of Materials Science and Engineering in NPU.

References

- Hirano K. Application of eutectic composites to gas turbine system and fundamental fracture properties up to 1700 °C. *J Eur Ceram Soc* 2005;**25**:1191–9.
- Bei H, George EP. Microstructures and mechanical properties of a directionally solidified NiAl–Mo eutectic alloy. *Acta Mater* 2005;**53**:69–77.
- Triveño RC, Oliveira MF, Caram R, Botta FWJ, Bolfarini C, Kiminami CS. Directional and rapid solidification of Al–Nb–Ni ternary eutectic alloy. *Mater Sci Eng A* 2004;**375–377**:565–75.
- Waku Y, Nakagawa N, Wakamoto T, Ohtsubo H, Shimizu K, Kohtoku Y. A ductile ceramic eutectic composite with high strength at 1873 K. *Nature* 1997;**389**:49–52.
- Sayir A, Farmer SC. The effect of the microstructure on mechanical properties of directionally solidified $\text{Al}_2\text{O}_3/\text{ZrO}_2(\text{Y}_2\text{O}_3)$ eutectic. *Acta Mater* 2000;**48**:4691–7.
- Llorca J, Orera VM. Directionally solidified eutectic ceramic oxides. *Prog Mater Sci* 2006;**51**:711–809.
- Oliete PB, Peña JI, Larrea A, Orera VM, Llorca J, Pastor JY, et al. Ultra-high strength nanofibrillar Al_2O_3 –YAG–YSZ eutectics. *Adv Mater* 2007;**19**:2313–8.
- Mazerolles L, Perriere L, Lartigue-Korinek S, Piquet N, Parlier M. Microstructures, crystallography of interfaces, and creep behavior of melt-growth composites. *J Eur Ceram Soc* 2008;**28**:2301–8.
- Waku Y, Nakagawa N, Wakamoto T, Ohtsubo H, Shimizu K, Kohtoku Y. The creep and thermal stability characteristics of a unidirectionally solidified eutectic composite. *J Mater Sci* 1998;**33**:4943–51.
- Orera VM, Merino RI, Pardo JA, Larrea A, Fuente G, Contreras L, et al. Oxide eutectics: role of interfaces in the material properties. *Acta Phys Slovaca* 2000;**50**:549–57.
- Ochiai S, Ueda T, Sato K, Hojo M, Waku Y, Nakagawa N, et al. Deformation and fracture behavior of an $\text{Al}_2\text{O}_3/\text{YAG}$ composite from room temperature to 2023 K. *Comp Sci Tech* 2001;**61**:2117–28.
- Park D-Y, Yang J-M. Fracture behavior of directionally solidified CeO_2 - and Pr_2O_3 -doped $\text{Y}_3\text{Al}_5\text{O}_{12}/\text{Al}_2\text{O}_3$ eutectic composites. *Mater Sci Eng A* 2002;**332**:276–84.
- Peña JI, Larsson M, Merino RI, de Francisco I, Orera VM, Llorca J, et al. Processing, microstructure and mechanical properties of directionally-solidified Al_2O_3 – $\text{Y}_3\text{Al}_5\text{O}_{12}$ – ZrO_2 ternary eutectics. *J Eur Ceram Soc* 2006;**26**:3113–23.
- Calderon-Moreno JM, Yoshimura M. Al_2O_3 – $\text{Y}_3\text{Al}_5\text{O}_{12}(\text{YAG})$ – ZrO_2 ternary composite rapidly solidified from the eutectic melt. *J Eur Ceram Soc* 2005;**25**:1365–8.

15. Su HJ, Zhang J, Cui CJ, Liu L, Fu HZ. Rapid solidification of $\text{Al}_2\text{O}_3/\text{Y}_3\text{Al}_5\text{O}_{12}/\text{ZrO}_2$ eutectic *in situ* composites by laser zone remelting. *J Cryst Growth* 2007;**307**:448–56.
16. Oliete PB, Peña JI. Study of the gas inclusions in $\text{Al}_2\text{O}_3/\text{Y}_3\text{Al}_5\text{O}_{12}$ and $\text{Al}_2\text{O}_3/\text{Y}_3\text{Al}_5\text{O}_{12}/\text{ZrO}_2$ eutectic fibers grown by laser floating zone. *J Cryst Growth* 2007;**304**:514–9.
17. Nagira T, Yasuda H, Takeshima S, Sakimura T, Waku Y, Uesugi K. Chain structure in the unidirectionally solidified Al_2O_3 –YAG– ZrO_2 eutectic composite. *J Cryst Growth* 2009;**311**:3765–70.
18. Waku Y, Sakata S, Mitani A, Shimizu K. Temperature dependence of flexural strength and microstructure of $\text{Al}_2\text{O}_3/\text{YAG}/\text{ZrO}_2$ ternary melt growth composite. *J Mater Sci* 2002;**37**:2975–82.
19. Su HJ, Zhang J, Tian JJ, Liu L, Fu HZ. Preparation and characterization of $\text{Al}_2\text{O}_3/\text{Y}_3\text{Al}_5\text{O}_{12}/\text{ZrO}_2$ ternary hypoeutectic *in situ* composite by laser rapid solidification. *J Appl Phys* 2008;**104**, 023511–1–7.
20. Harada Y, Uekawa N, Kojima T, Kakegawa K. Formation of $\text{Y}_3\text{Al}_5\text{O}_{12}$ – Al_2O_3 eutectic microstructure with off-eutectic composition. *J Eur Ceram Soc* 2008;**28**:1973–8.
21. Barclay RS, Kerr HW, Niessen P. Off-eutectic composite solidification and properties in Al–Ni and Al–Co alloys. *J Mater Sci* 1971;**6**:1168–73.
22. Harada Y, Uekawa N, Kojima T, Kakegawa K. Fabrication of dense material having homogeneous GdAlO_3 – Al_2O_3 eutectic-like microstructure with off-eutectic composition by consolidation of the amorphous. *J Eur Ceram Soc* 2009;**29**:2419–22.
23. Su HJ, Zhang J, Liu L, Fu HZ. Microstructure and mechanical properties of a directionally solidified $\text{Al}_2\text{O}_3/\text{Y}_3\text{Al}_5\text{O}_{12}/\text{ZrO}_2$ hypoeutectic *in situ* composite. *Comp Sci Tech* 2009;**69**:2657–67.
24. Larrea A, Fuente GF, Merino RI, Orera VM. ZrO_2 – Al_2O_3 eutectic plates produced by laser zone melting. *J Eur Ceram Soc* 2002;**22**:191–8.
25. Ester FJ, Merino RI, Pastor JY, Martín A, Llorca J. Surface modification of Al_2O_3 – ZrO_2 (Y_2O_3) eutectic oxides by laser melting: processing and wear resistance. *J Am Ceram Soc* 2008;**91**:3552–9.
26. Lakiza SM, Lopato LM. Stable and metastable phase relations in the system alumina–zirconia–yttria. *J Am Ceram Soc* 1997;**80**:893–902.
27. Su HJ, Zhang J, Cui CJ, Liu L, Fu HZ. Growth characteristic of $\text{Al}_2\text{O}_3/\text{Y}_3\text{Al}_5\text{O}_{12}$ (YAG) eutectic ceramic *in situ* composites by laser rapid solidification. *J Alloys Compd* 2008;**456**:518–23.
28. Echigoya J, Takabayashi Y, Sasaki K, Hayashi S, Suto H. Solidification microstructure of Y_2O_3 -added Al_2O_3 – ZrO_2 eutectic. *Trans Jpn Inst Metals* 1986;**27**:102–7.
29. Calderon-Moreno JM, Yoshimura M. Microstructure and mechanical properties of quasi-eutectic Al_2O_3 – $\text{Y}_3\text{Al}_5\text{O}_{12}$ – ZrO_2 ternary composites rapidly solidified from melt. *Mater Sci Eng A* 2004;**375–377**:1246–9.
30. Larrea A, Orera VM, Merino RI, Peña JI. Microstructure and mechanical properties of Al_2O_3 –YSZ and Al_2O_3 –YAG directionally solidified eutectic plates. *J Eur Ceram Soc* 2005;**25**:1419–1419.
31. Su HJ, Zhang J, Cui CJ, Liu L, Fu HZ. Rapid solidification behaviour of $\text{Al}_2\text{O}_3/\text{Y}_3\text{Al}_5\text{O}_{12}$ (YAG) binary eutectic ceramic *in situ* composites. *Mater Sci Eng A* 2008;**479**:380–8.
32. Polotai AV, Foreman JF, Dickey EC, Meinert K. Laser surface processing of B_4C – TiB_2 eutectic. *Int J Appl Ceram Technol* 2008;**5**:610–7.
33. Flemings MC. *Solidification processing*. New York: McGraw-Hill, Inc.; 1974.
34. Sato T, Sayama Y. Completely and partially co-operative growth of eutectics. *J Cryst Growth* 1974;**22**:259–71.
35. Bei H, George EP, Kenik EA, Pharr GM. Directional solidification and microstructures of near-eutectic Cr– Cr_3Si alloys. *Acta Mater* 2003;**51**:6241–52.
36. Mizutani Y, Yasuda H, Ohnaka I, Maeda N, Waku Y. Coupled growth of unidirectionally solidified Al_2O_3 –YAG eutectic ceramics. *J Cryst Growth* 2002;**244**:384–92.
37. Čička R, Trnovcová V, Yu M, Bošák O. Microstructure and electrical properties of near-eutectic alumina–zirconia composites. *J Optoelectron Adv Mater* 2006;**8**:1460–5.